Typeset using LaTeX default style in AASTeX631

Measurement of the Kicker transient magnetic field in the Muon g-2 Experiment at Fermilab

NICOLA VALORI [1]

SUPERVISORS: MARCO INCAGLI & HOGAN NGUYEN,

[1] *University of Pisa, Pisa, Italy*

ABSTRACT

The Muon g-2 experiment at Fermilab has the main goal to measure the muon anomalous magnetic moment $a_\mu = \frac{g-2}{2}$ to a precision of 140 parts per billion (ppb), which means 4 times improvement in precision with respect to the final result from BNL:

$$a_\mu(expt.BNL) = 11659208.0(6.3) \times 10^{-10} \ (540\ ppb)$$

So far only RUN1 data have been analyzed showing the following improvement:

$$a_\mu(expt.RUN1) = 116592061 \times 10^{-11} \ (465\ ppb)$$

In this report I summarize the work done at the g-2 experiment during my summer internship at Fermilab where I worked on the attempt to estimate the kicker transient field contribution in the Muon g-2 experiment.

1. INTRODUCTION

In this report, I focus on RUN 2 and 3 of the E989 experiment, showing, after a brief introduction, the steps I carried on in order to study the eddy currents effect arising after kicks. In the E989 experiment, 3.1 Gev muons beams are injected into a 14 m diameter storage ring (SR), where both muon's spin and momentum vectors precede. The difference between the spin frequency and the cyclotron frequency is called "anomalous precession frequency", related to a_μ through $\omega_a = a_\mu \frac{q}{m} B$, where B is the magnetic field inside the SR. Therefore, a_μ can be extracted by accurately measuring ω_a and B.

In particular we are interested in Kickers' region that is located at 3 o' clock respect to the injector region as we can see from the picture.

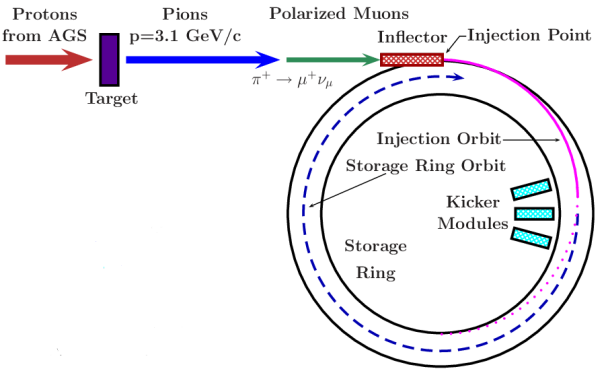

Figure 1. SR schematic: the blue dashed line represents muons path inside the ring

Once muons come into the ring, they need to be placed in the correct orbit before starting to properly turn. For this aim, a system of three kickers produces a 200-300 G magnetic field parallel to the ring field that steers the muon beam onto the designed orbit. In order to understand the issues that come from this process, we need to describe how kickers work and,in

doing so, I will use some plots deriving from my analysis.

2. KICKERS ROLE

A series of three 1.27-m-long non-ferric aluminum kicker electromagnets are placed a quarter of the betatron wavelength from the inflector to reduce the impact of the ring magnetic field when they are pulsed with ~4 kA. The result of the localized perturbation moves muons onto stable orbits that facilitate a measurement of a_μ. Likewise, the use of non-ferric materials was explicitly selected to not affect the a_μ measurement, which is sensitive to magnetic field sources. Beam arrives in a bunch train of 120 ns pulses at an instantaneous rate of 100 Hz (11.4 Hz average), and each bunch propagates around the ring every 149.2 ns. The kicker current must support the full duration of each beam pulse and ideally ceases before the muons make one full revolution of the ring. To address these timing specifications, Blumlein pulse forming networks (PFNs) were selected to drive the kicker currents at FNAL. A more detailed description of the kickers system can be found in (1).

Roughly speaking, Blumlein system can be descibed as a sort of capacitor in which we can observe the charge-discharge phenomenon.

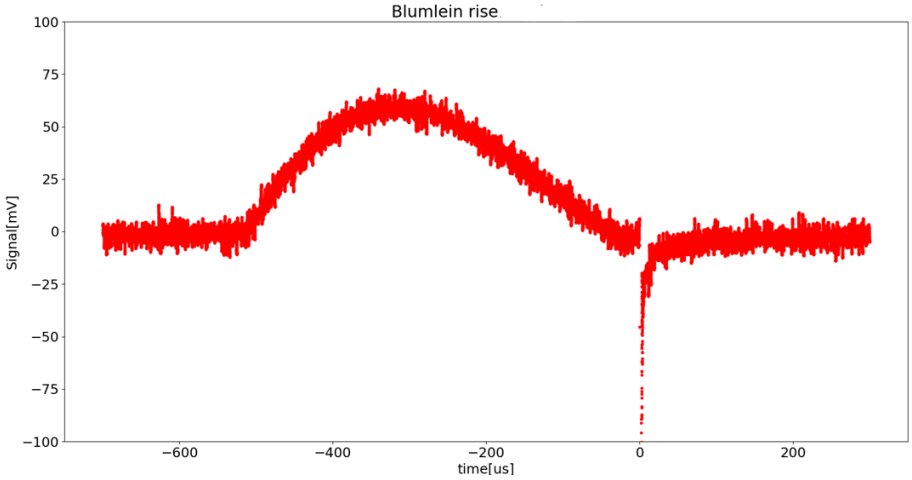

Figure 2. Charge and discharge of the Blumlein

As we can see in Fig.2, there is a spike at the end of the Blumlein fall: basically, this is what we means when we say "kick". Kicks last only ~ 100 ns and for this reason they produce eddy currents, and hence, a spurious magnetic field which affect the measurements of ω_a. This is due to two aluminium plates which are placed inside the ring in correspondence of kickers' cage. Despite the fact that the magnetic field generated by this eddy currents is pretty small compared to the one used to put the mouns in their orbits (1.45 T), it affects our results of -27(37) ppb during the RUN 1 (2).

As the FNAL final goal is to reach a precision of 140 ppb, also this measure is playing a key role in a_μ calculus. Two teams are currently working at Fermilab in order to improve previous measurement. Both of them work using magnetometers which are based on Faraday effect rotation: a fiber magnetometer, built at the Argonne National Laboratory and an independent device, built on a breadboard and based on the same principle but with different characteristics, has been built by INFN.

During summer 2022 I worked with the second one with the help of the INFN team in order to measure the effect due to residual eddy currents.

3. THE INFN MAGNETOMETER

As mentioned above, the INFN magnetomer works with Faraday rotation effect, a particular property of some materials. Faraday roation effect occurs when a material with a magnetic field inside is crossed by a light beam. Generally speaking, a linearly polarized laser beam with a fixed polarization comes out from the material with a different one.

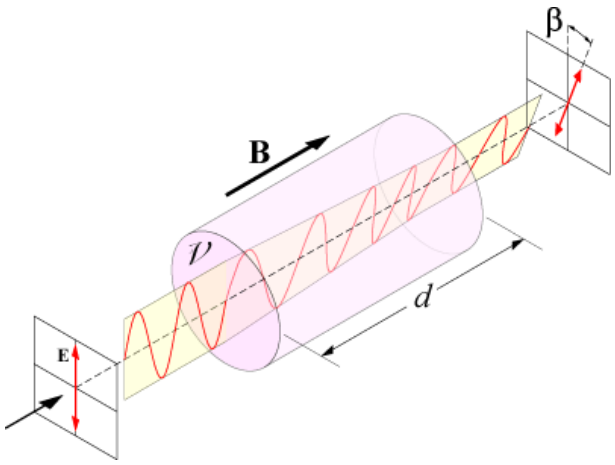

Figure 3. Faraday rotation effect

Fig.3 describes in very clear way the mechanism behind this process. The rotation is based on a linear equation which links together the rotation angle and the field.

$$\theta = BVd \tag{1}$$

Let me descirbe term by term Eq.1.

- θ: the angle of rotation (in radians)
- B: the magnetic field inside the crystal in the direction of the light propagation (in teslas)
- d: the length of medium traversed (in meters) where the light and magnetic field interact
- V: the Verdet constant for the material. This empirical proportionality constant (in units of radians per tesla per meter) varies with both frequency and temperature, and it is tabulated for various materials.

In our experiment the crystal chosen is made of TGG (Terbium Gallium Garnet), which has a reported Verdet constant of -131 rad T^{-1} m^{-1}. Another detail that has to be underlined is the crystal lenght: we choose d such that, for a 1.45 T magnetic field, the rotation angle is a multiple of 2π in order to avoid further rotation.

As we will see later, working with the magnetic field on is a pretty difficult challenge and the correct setting of the all parameters can be crucial.

Let's move on the description of INFN Breadboard, the magnetometer used this summer in order to achieve our goal.

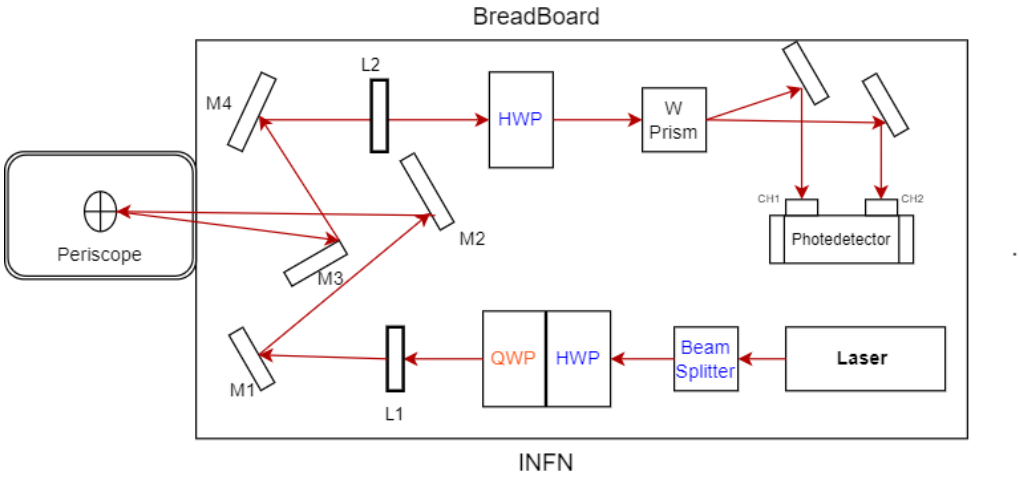

Figure 4. Schematic of the breadboard and laser path

Before starting with the description of the breadboard function, let me focus on the list of components:

- Linearly polarized red light laser
- A Beam splitter is used to improve the signal and also to measure the power lost by the laser beam (thanks a powermeter)
- Dieletric mirrors
- The first Half Wave Plate(HWP) is used to maximize the signal once it gets out of the beam splitter.
- A Quarter Wave Plate(QWP) is used to study the noise and it is not required during the Data acquisition
- A Periscopes system is composed by two TGG crystall and it will be describe in a better way later.
- Two focusing lenses with f = 750 mm and f = 200 mm.
- The second Half Wave Plate is used to balance the signal before the acquisition
- A Wollaston Prism is used to split laser light in two beams with a defined angles
- Photodetector collects signals and gives first beam, second beam and the difference output intensities

The laser path is shown in Fig.4 and it is quite simple to understand the mechanism.

The main device is the periscope. Actually, in our measurement session we used two different periscopes, one with a lens and another without lens. The periscopes structure has several improvements from the June one and all of them led us to a better work. Also in this case a list is required to show you in more direct and comprehensive way the components of the periscope structure.

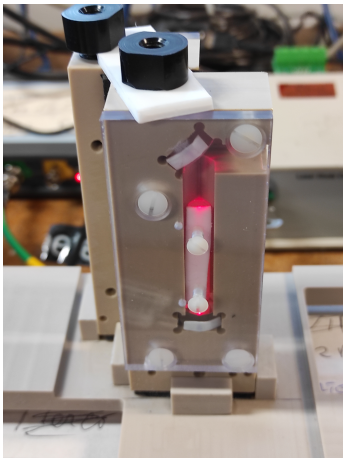

Figure 5. Persicope picture: On the top the first mirror, the crystal in the middle and at the bottom the second mirror

- A plastic Bridge is used to reduce the mechanical vibrations after kicks
- The unlensed periscope is a structure composed by a TGG crystal which is inserted between two mirrors
- The lensed crystal has the same structure of the unlensed one but a lens should help us to reduce the mechanical vibrations effects
- A Teflon bar is place at the top in order to connect better the two periscope: it also give a better stability to the whole structure.

Making a summary of the breadboard mechanism, the light hits a first mirror at the top of a periscope, the mirror deflects the light and it crosses the TGG crystal: if a magnetic field is turned on,the polarization rotates and, after it has hit a second mirror,crosses the periscope a second time before coming back. So, in total we have two Faraday rotation. Once this is done, the light gets out and follows the path described in Fig.4 in order to get into a Wollaston prism and, subsequently, to be collected by the two photodiodes. At the start, the second HWP is used to set the difference between the two signals equal to 0. In this way, once the polarization changes, we will be able to see an output signal different from 0.

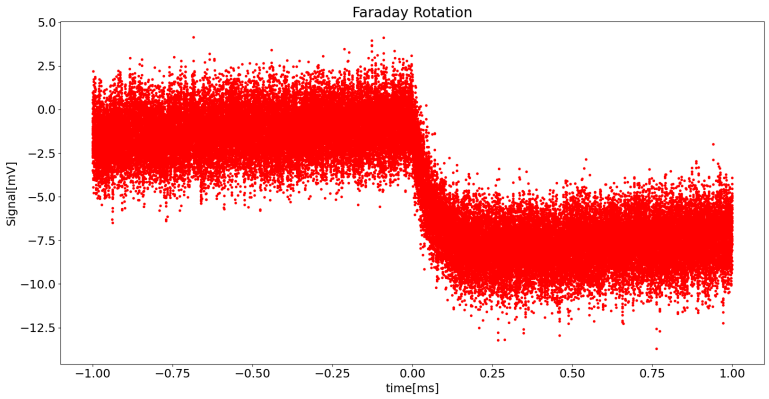

Figure 6. Description of the Faraday effect: The picture shows signal difference between the two photodetector channels. For B = 0 we have an up signal equal to 0. For B≠ 0 we have a signal ≠ 0

4. HARDWARE ACTIVITIES

One of the most important steps of this work consist on the set up of the framework. As a matter of fact our measures depend on the level of accuracy of the setting and, for this reason, a large part of the work is focused on the hardware. First of all, we have to put the periscope inside the ring. In doing so we have to open the kicker number 3 window and place the structure between the aluminium plates: the difficulty of this work is due to the narrowness of the working environment.

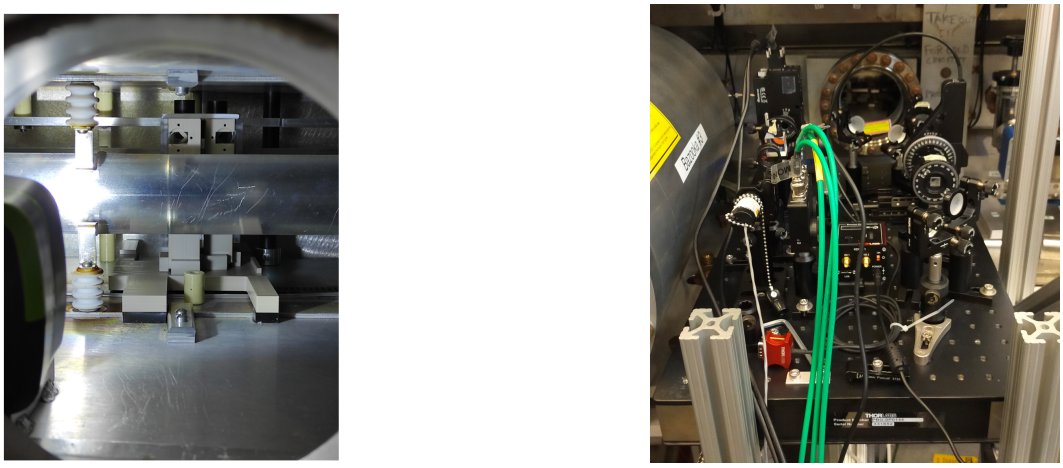

(a) (b)

Figure 7. Fig.7(a):Periscope inside the ring. Fig.7(b): the INFN breadboard mounted in kicker 3 cage

After that, the breadboard is moved into the ring hall and it has been mounted in the kicker number 3 cage. Pictures describing these steps are Fig.7. Once that is done we have to reproduce experimental work environment, the one used during the RUNs and it consists on three settings: to make vacuum inside the ring,to turn on the magnetic field, to configure

kicker 3. To turn on the main magnetic field is necessary to ramp up the current slowly and, as I explain subsequently, this can give us some information regards the calibration Volt-Gauss. Kicker is set at 42 kV because we want to work with RUN 2 and RUN 3 parameters.

The largest part of the work is the laser alignment. Despite the fact that the laser path can be appear easy, directiong it using mirrors and lens is not so trivial: millimeters make the difference between a good alignment and a bad one. Paolo Girotti[1] and I found an useful pattern to make alignments and it can be summarized with the following steps.

- Don't use any cameras.Although helpful to look at the beam positioning in the crystal,reflection completely blind the view
- Move the farthest mirror(M3 in Fig.4) in order to have a better view
- Center the beam into the periscope. Observe the return beam spot and move return beam halfway in that direction, both vertically and horizontally. Main goal is to have return beam ~2 mm toward the left of the incoming beam.
- Insert M3 mirror in order to align return beam
- Check signals using Picoscope[2]

Despite the simple description, this process lasted hours because of the difficulty to understand where the beam spot actually is. Indeed there were a lot of reflections due to kicker's window and other components that made Paolo and I puzzled on where was the main spot. Although the last point of the list above may seem pointless, it is fundamental because main errors were based on a wrong evaluation of the real beam spot.

5. HWP AND QWP SCAN

Before starting every acquisition, a scan over HWP and QWP angles is required. The plates can be regulated remotely thanks to a software named *Kinesis*.

The scan consist on choosing a large angles range and measuring the Blumlein peak for each angle, in order to find the best trade off between signal amplitude and signal over noise ratio. Then, we plot signal vs angles to select a peak. Once doing that, we repeat the scan more carefully in a region around a selected peak. The acquisition setting for each angle is the following:

- Kicker 3 at 42 kV
- 512 traces
- 1 ms interval
- 62505 points for each sample

Thanks to a *Python* software it has been possible to analyze each angle in a very fast way. Giving Data to my program it performs the following steps to get baseline, peak and amplitude:

- It selects the first 10% and the last 20% of the sample and then performs average and standard deviation to obtain baseline value
- Select between 30% and 45% of the sample and perform a parabolic fit with Fit function: a + c*((x-b)**2) in order to obtain the peak.
- Subtract peak and Baseline in order to obtain the rise

It has to be underlined that this process is done only for the first kick. The original idea was to trigger using C channel of the picoscope (the one that gives the difference as output between channels amplified by 28) in order to use the kick itself as trigger: in this way we could take in account of each kick. However we found the picoscope is not enough fast to take all kicks and so only the first has been analyzed for this measure.

[1] Pisa University PhD student who worked with me during the first days of my stay at Fermilab

[2] The software we used during the analysis

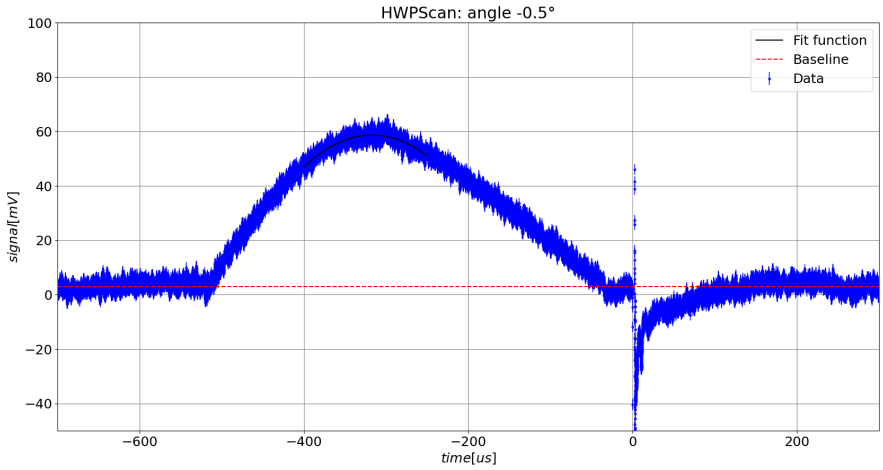

Figure 8. Example plot for -0.5° angle: In blue are shown data, in red dashed line the baseline iìI found and in black fit function in its fit interval

After that we can choose the best angle plotting signal vs angle and single over noise vs angle. For the noise we consider the baseline standard deviation.

6. MAGNET RAMP UP: THE CALIBRATION

In this section I will explain how we can calibrate the mV to mG conversion using the magnet ramp up. We need to turn on the magnet from 0 to 1.45 T with a current that slowly increase from 0 to 5173 A. We can collect the signal difference between the two channel in function of the current. As we expected, we have another way in which Faraday rotation effect manifests itself. As a matter of fact, with the increasement of the magnetic field, the light polarization rotates periodically outlining a sinusoidal shape.

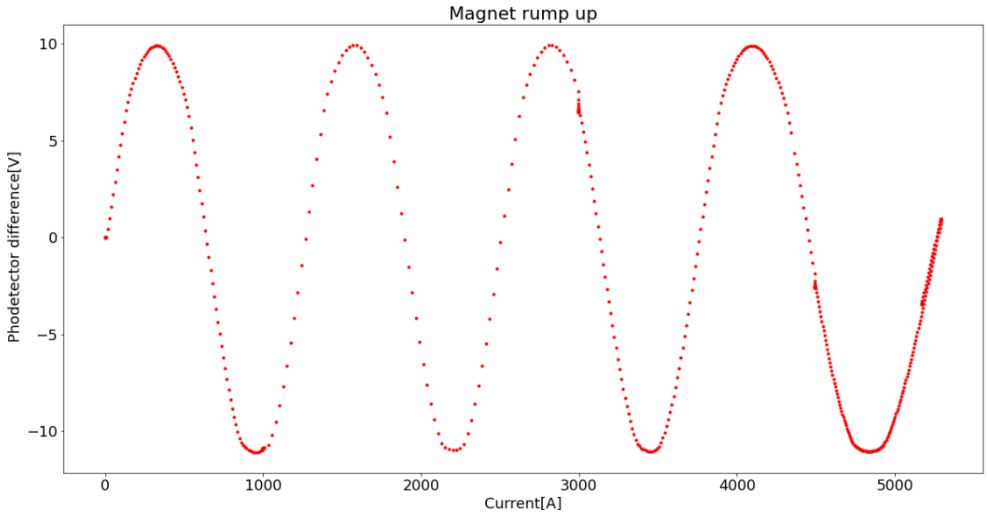

Figure 9. Caption

How can we get information on the calibration from this plot?

As mentioned above we have a sinusoidal shape so, around a 0 point, we can perform a Taylor expansion to find a linear correlation between Volt and Ampere. In doing so I arbitrarily selected 4 points around 0 and performed a linear fit.

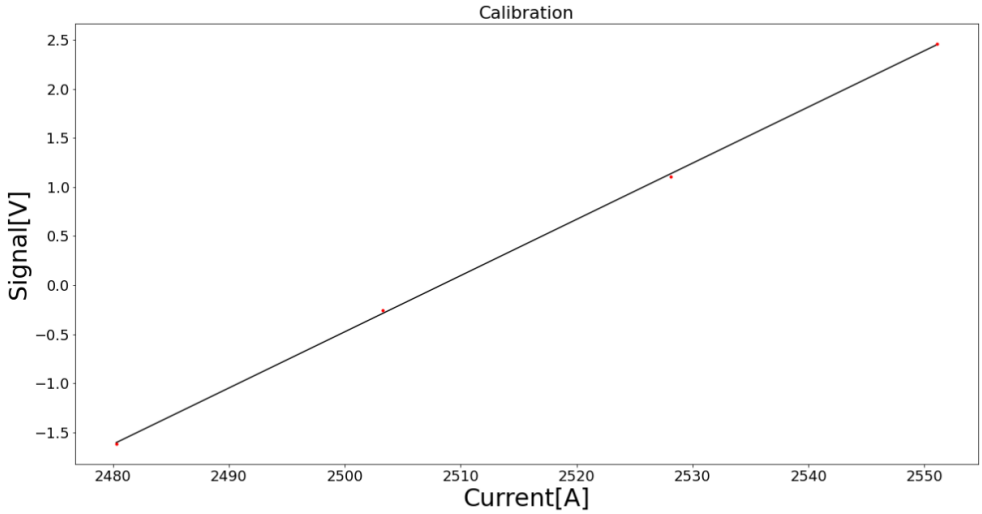

Figure 10. Caption

Fitting with the following fit function:

$$offset + c * x$$

It turns out to be c = 0.057315 ± 0.000009 mV/mA. Because we are interested in mG calibration we can exploit the fact that for a 5173 A current we have a 1.45 T magnetic field. Furthermore in our analysis we always used the difference between the two channels amplified by a 28 factor. So in order to use our calibration properly, we have to multiply by 28. The final result is c = 0.57253 ± 0.00009 mV/mG.

7. LONG ACQUISITION

Our goal is to measure eddy currents contribution both for lensed and unlensed periscope and we repeat all steps previously described twice.

Once everything is done we can start a long acquisition lasting several hours. The general setting used for both periscopes is the following:

- no QWP
- 500 ksample
- 138 traces
- time interval: 100 ms

Our first idea was to use QWP to study the noise but we were not able to nullify the Faraday rotation effect with the magnetic field on. The noise study is not easy to manage and several attempts have been done but, for the moment, we have not found a solution.

As mentioned in previous sections we have 8 kicks separated by 10 ms so we selected a 100 ms trace that starts using the T9 as trigger.

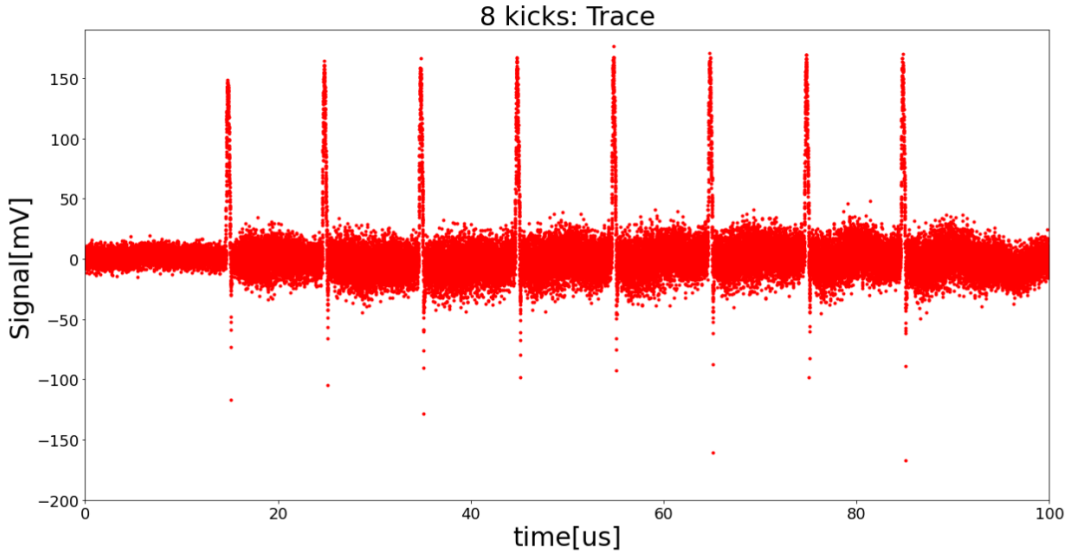

Figure 11. Trace of the all 8 kicks acquisition

In Fig. 11 we can see the Blumlein rise and fall that precedes each kick and, at the end, kick's spike who fall down hastily before the eddy currents rise.

8. DATA ANALYSIS

The steps followed for both periscopes are essentially the same. First of all I made a rebin of 10 for all data and then I performed an exponential fit.

In general the large part of FNAL work is focused on the ω_a fit that is defined as the difference between momentum and spin frequency. The fact that this difference is different from 0 led us to the conclusion that g must not be equal to 2.

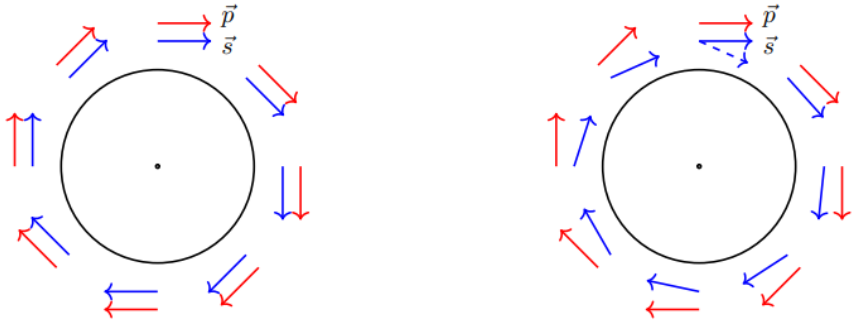

Figure 12. Illustration of the motion of the muon spin and momentum vectors for a muon orbiting in a magnetic field when g = 2, so the spin does not rotate relatively to the muon momentum, and when g > 2 [21]

The law behind the description of this fact is:

$$\vec{\omega_a} = \frac{q}{m}\left[a_\mu \vec{B} - a_\mu\left(\frac{\gamma}{\gamma+1}\right)(\vec{\beta}\cdot\vec{B})\vec{\beta} - \left(a_\mu - \frac{1}{\gamma^2-1}\right)\frac{\vec{\beta}\times\vec{E}}{c}\right]$$

As we can easily see there is the presence of a magnetic field that will be affected by eddy currents. For this reason we want to analyze eddy currents effect in the temporal window between 30 μs and 700 μs after the kick, that is the same of the ω_a fit. I followed the strategy of (2), where it is used the following fit function:

$$\Delta B = offset + B_{EC}e^{-\frac{(t-0.03)}{\tau}}$$

8.1. *Unlensed periscope*

The first analysis performed is the one with the unlensed periscope. We removed QWP because it was not essential in this part of the project and we performed a first HWP scan. After that, a more fine scan led us to choose α = -0.5° as the best angle. This angle has an amplitude around 60 mV and a signal over noise ratio greater than 25.

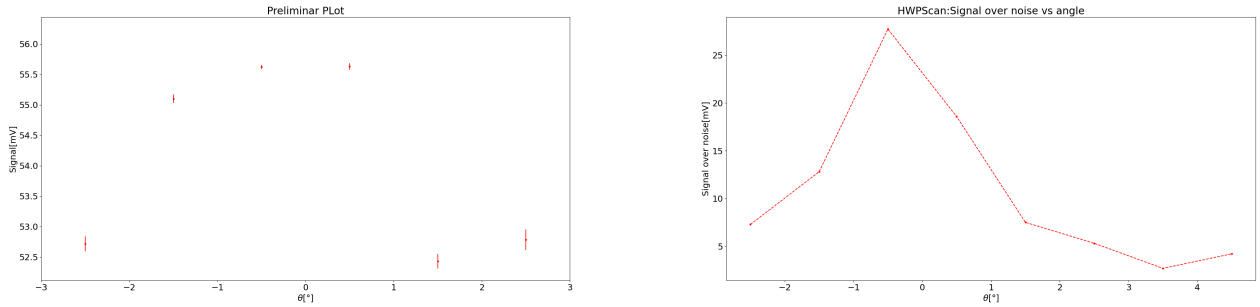

(a) (b)

Figure 13. Fig.13(a):Signal vs angle plot. Fig.13(b):Signal over noise vs angle plot

From that we can performed an exponential fit:

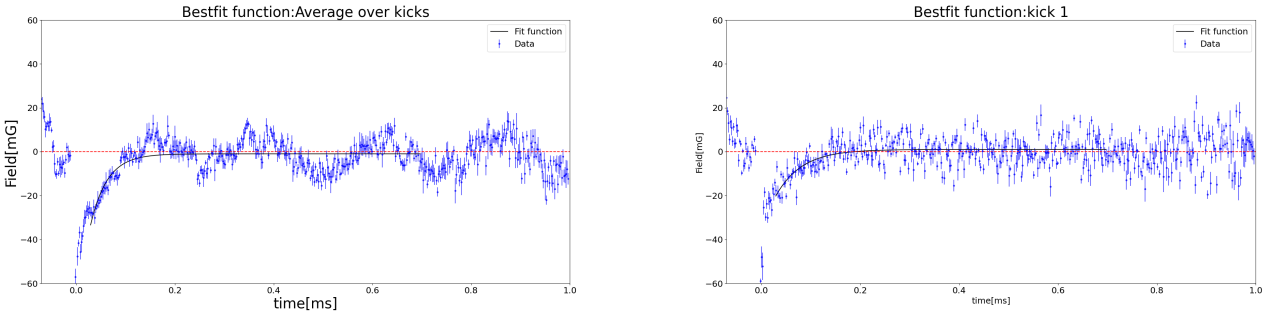

(a) (b)

Figure 14. Fig.14(a):kicks' average. Fig.13(b):first kick

We are mainly interested in the average over kicks and in the first kick: this is due to the fact that mechanical vibrations are lesser relevant than for the other kicks.

8.2. *Lensed periscope*

The second data analysis collection regards the lensed periscope where we repeated the same steps. However in this case we were not so lucky because the scan over HWP was trickier. We chose α = 55° that has an amplitude around 70 mV but a signal over noise ratio of only ~ 6.

This fact, as we can imagine, will lead us to a noisier data.

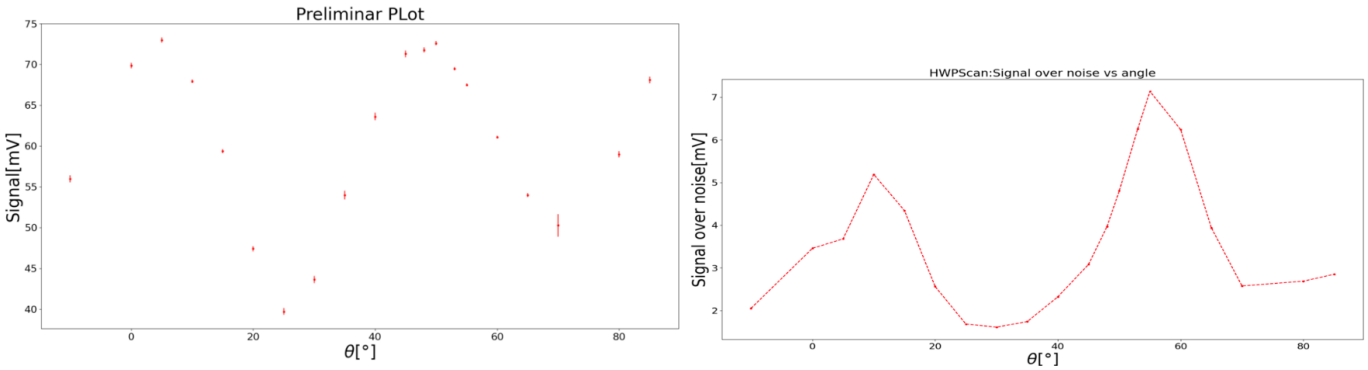

(a) (b)

Figure 15. Fig.13(a):Signal vs angle plot. Fig.13(b):Signal over noise vs angle plot

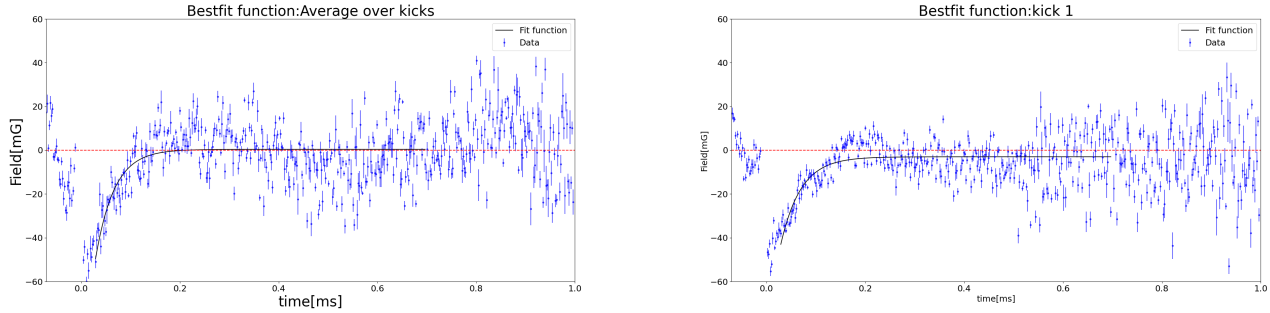

(a) (b)

Figure 16. Fig.14(a):kicks' average. Fig.13(b):first kick

We can see a great difference between the two periscopes. That is mainly due to our angle selection and to our impossibility to improve signal over noise ratio for the second periscope.

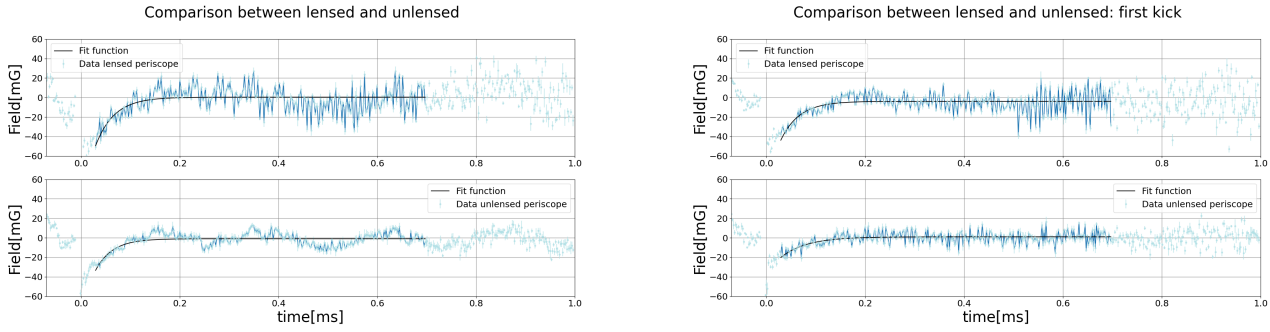

(a) (b)

Figure 17. Fig.14(a):kicks' average: comparison between unlensed and lensed periscope. Fig.13(b):first kick:comparison between unlensed and lensed periscope.

So far we have analyzed the data without any correction but we can improve our results starting from the observation of the previous naif fit.

Let's describe the two changes done;

- Remove baseline oscillation in order to get same baseline for each kick
- Remove mechanical oscillation

9.1. *Baseline oscillation*

From a trace plot we can notice that the baseline is not the same for each kick, in fact it makes an oscillation with a frequency ~ 20 Hz. This fact affects the results in two different way. First of all the average over all 8 kicks becomes inaccurate, secondly, making a comparison between kicks could be meaningless.

So, in order to get baseline oscillation, we remove from the trace, the points regarding blumlein rises and kicks and perform a sinusoidal fit over the whole trace.

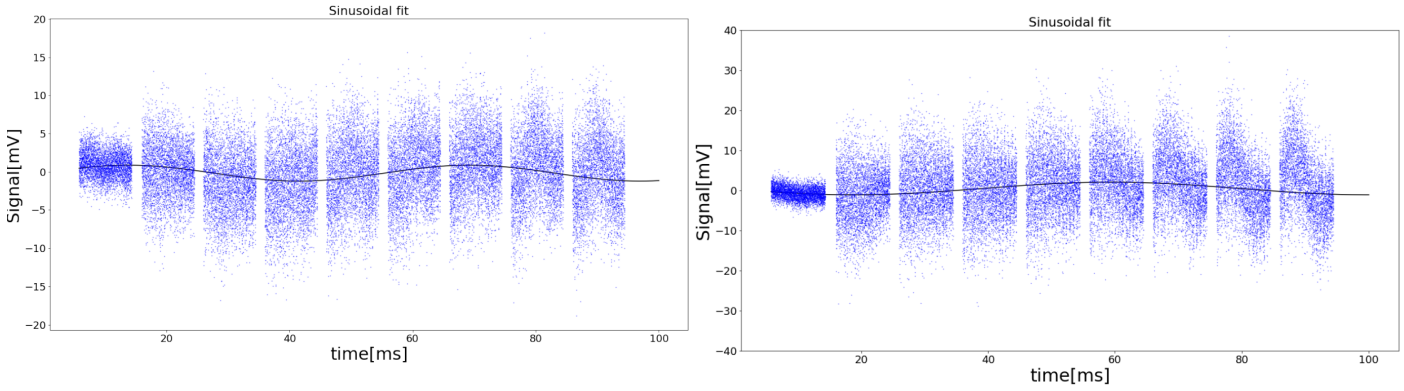

(a) (b)

Figure 18. Fig.17(a):Sinusoidal baseline fit for unlensed periscope . Fig.17(b):Sinusoidal baseline fit for lensed periscope

Last part of the work consist on subtract point by point the oscillation from the original data.

However this oscillation is very small and doesn't affect the analysis in a very relevant way. The crucial correction is the one we will describe in the next section

9.2. *Mechanical oscillation*

At a glance, from Fig.14 and Fig.16, we can see oscillations at the end of each kick. This fact is due to mechanical vibrations of the periscope and, despite the plastic bridge at the bottom of periscopes structure, they are still unavoidable. We can analyze and remove them a posteriori fitting a sinusoidal function between 0.1 and 1 ms after each kick and subtract the oscillation from the original data.

Despite the fact the experimental framework is essentially the same both for unlensed and lensed periscope, a difference has to be underlined. In fact while for the unlensed periscope we see only one main frequency, for the lensed one we notice two different modes of oscillation. This is more clear plotting the *Fast Fourier Trasform* of exponential fit residuals.

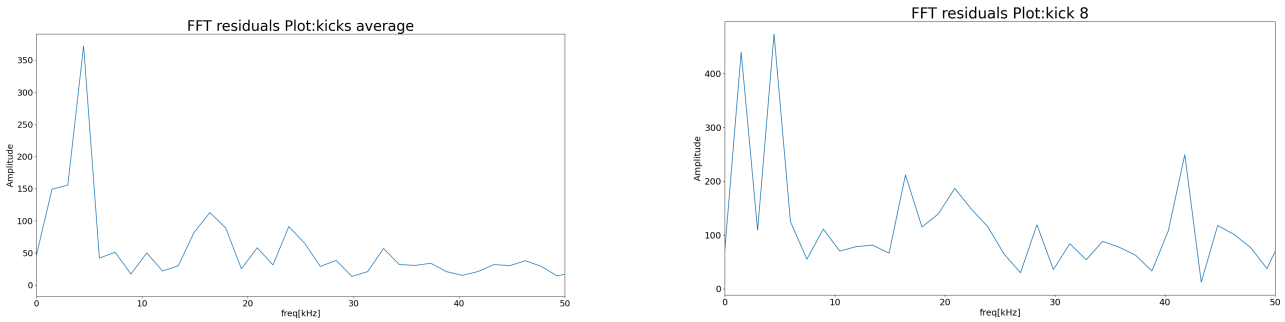

(a) (b)

Figure 19. Fig.19(a):Example plot of the FFT of exponential fit residuals for unlensed pericospe. Fig.19(b):Example plot of the FFT of exponential fit residuals for lensed pericospe

For the first periscope we basically follow the steps mentioned above only one time.

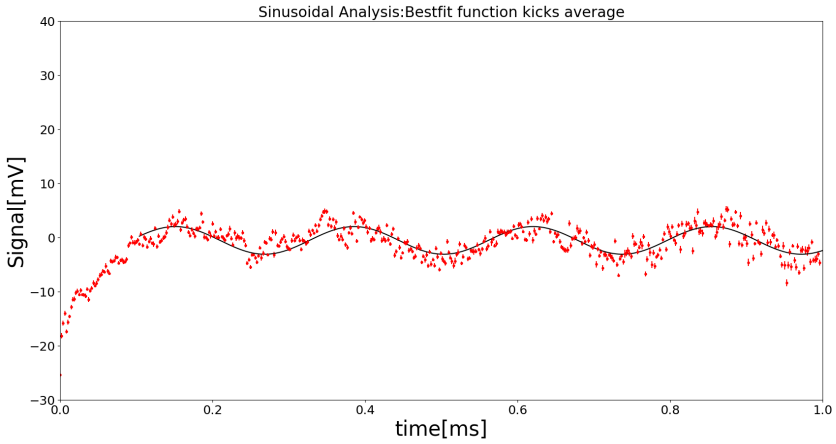

Figure 20. Example plot of data(red points) and the fit function(black line)

We found a ~ 4.5 kHz frequency for the kicks and it has been properly removed.

For the lensed periscope we have to remove two different frequencies. In doing so, we firstly fit and remove the main oscillation and then, starting from the new data, we fit and remove the second one.

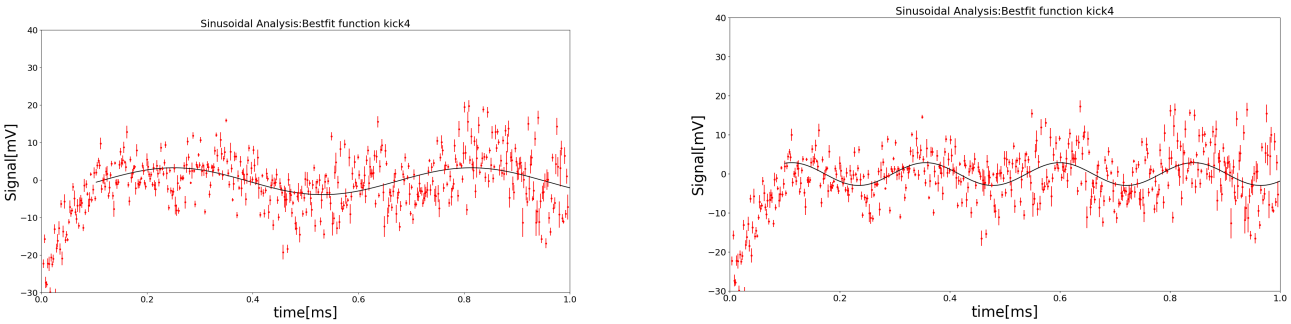

(a) (b)

Figure 21. Fig.21(a):Example plot of the data and fit function for data before any correction: we can see clearly a first frequency of ∼.1.6 kHz. Fig.19(b):Example plot of the data and fit function after having removed the first frequency: we can see the residual ∼ 4.5 kHz frequency

In this case, in addition to the 4.5 kHz frequency we can clearly see another frequency of ∼ 1.6 kHz.
Once this is done, our last task is to repeat the exponential fit with this new modified data.

10. SECOND FIT ATTEMPT

10.1. *Unlensed periscope*

The results of my second fit is more encouraging both for the clearness of the signal and for the comparison with RUN1 (we will see this aspect later).
I report fit function plots for the first periscope.

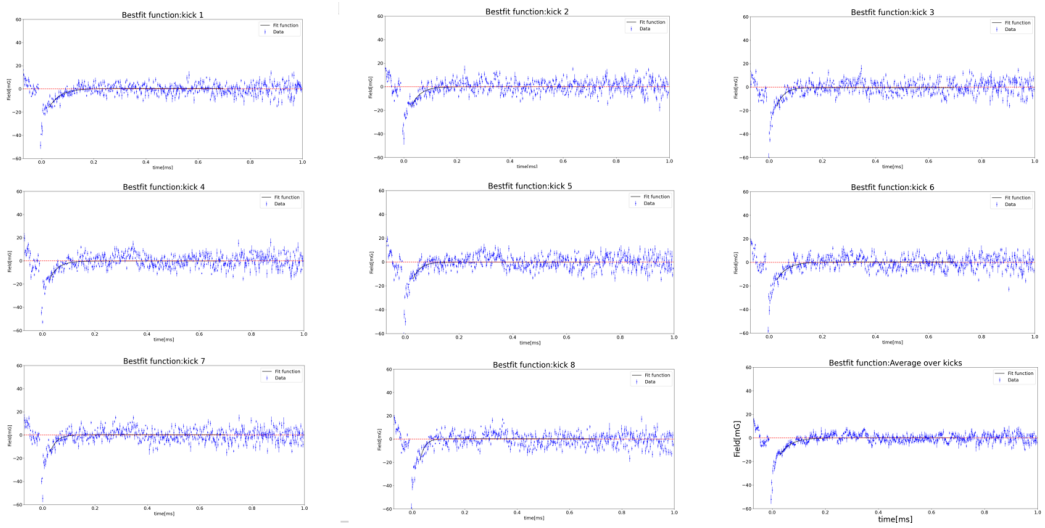

Figure 22. Plot for the 8 kicks and the average over kicks with exponential fit function for the unlensed periscope

The new Data are without a quite large period oscillation but, looking carefully at data plotted, it can be seen a further residual oscillation. From Fig.19(a), we notice a second lower peak around 17 kHz and several attempt in fitting this minor oscillation has been made.

Despite the fact we are not able to fit this frequency because of the background noise, we can convince ourselves of its existence also studying an easier framework.

Indeed, some data with magnetic field off has been collected as trial test for the functioning of the system and, with them, it has been possible to perform the sinusoidal fit, discovering that this mechanical vibration is actually present. For completeness I report also the fit function for this case, keeping mind that we are interesting in the phenomenon with magnetic field on, because that is the experimental framework during the RUNs.

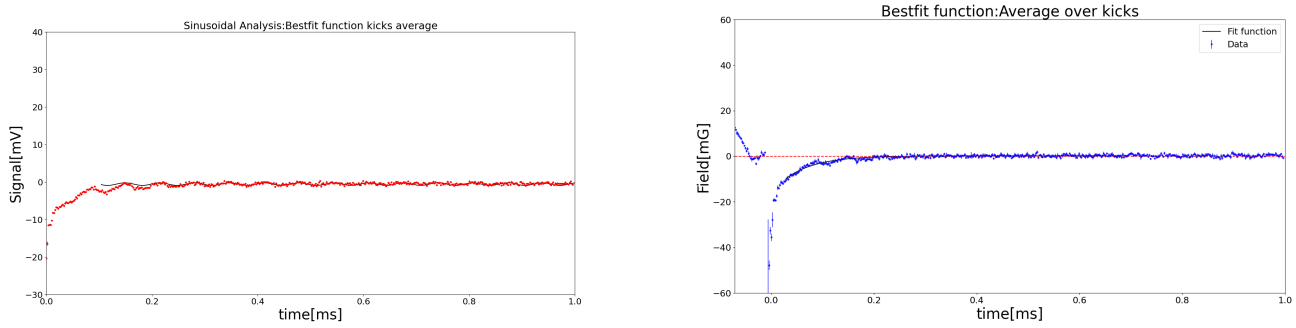

(a) (b)

Figure 23. Fig.23(a):Sinusoidal fit for data without magnetic field. Fig.23(b):Exponential fit for data without magnetic field after having removed the ~ 17 kHz frequency

In this test case the data plot is pretty flat and represents and ideal situation for an exponential fit. An improvement in breadboard system, maybe, could bring us to a noise reduction and so to a better evaluation of the eddy currents contribution.

10.2. *Lensed periscope*

Below, I report data plot for lensed periscope.

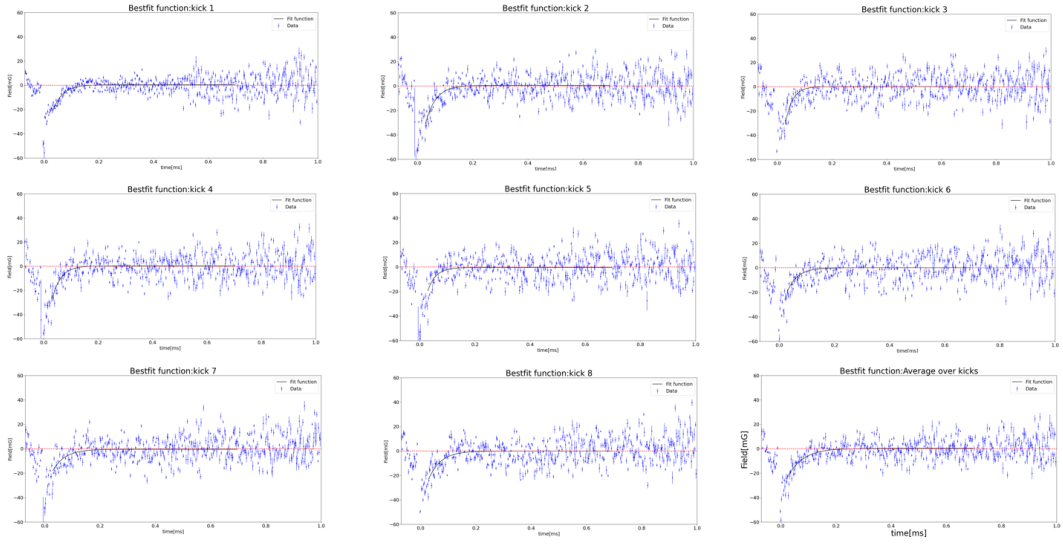

Figure 24. Plot for the 8 kicks and the average over kicks with exponential fit function for the lensed periscope

In this case further oscillations are not visible and we can't state if such a great noise is due to lens or a bad scan. We tested lensed periscope with the hope of clear our signal but we are not seeing any improvement on this side.

However, it has to be underlined how we was lucky with the other periscope: being the first one, we spent more time with it and we found a very good angle after several attempts. In this second time we had no much time and for this reason the HWP has been more superficial.

11. RUN1 COMPARISON

I am going to get my work down making a comparison with the only reference I had, namely, the RUN1 paper(2). In (2), the total uncertainty includes those from calibration, fit uncertainty, and background subtraction. It was estimated an uncertainty on the background subtraction of 6 mG. We would have liked to study the background subtraction also for our

data but for reason already explain that has not been possible. So the only thing I could do, was plotting my data and fit function considering RUN1 error bar.

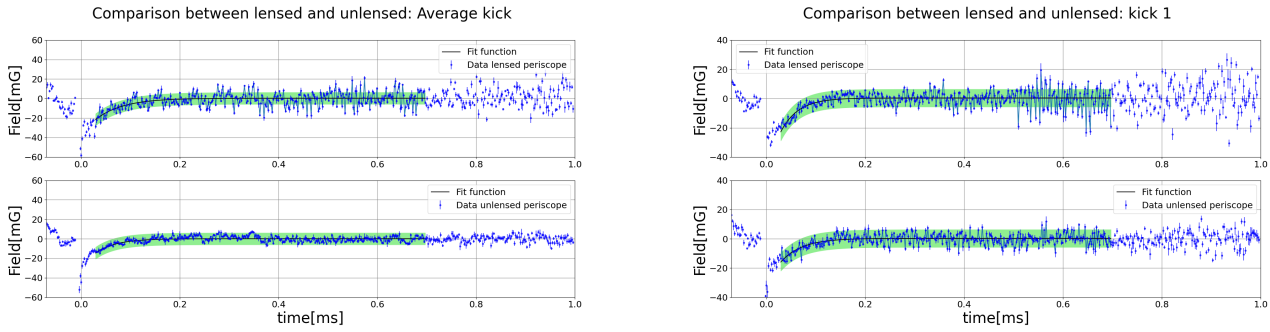

(a) (b)

Figure 25. Fig.25(a):Blue spots represent data, black line is the fit function and green region is the uncertainty used for RUN 1: kicks' average. Fig.25(b):Blue spots represent data, black line is the fit function and green region is the uncertainty used for RUN 1: first kick

Plots are self-explanatory and show a great consistency with RUN1 even if for the lensed periscope we expect a greater uncertainty.

Going beyond, we can compare each parameter with the RUN1 ones, which are:

$$offset = 0 \text{ (they fixed the offset)}$$

$$B_{EC} = (-18.7 \pm 2.5) \text{ mG}$$

$$\tau = (68 \pm 15)\ \mu\text{s}$$

A figurative way to compare is plotting a graph where all results are shown.

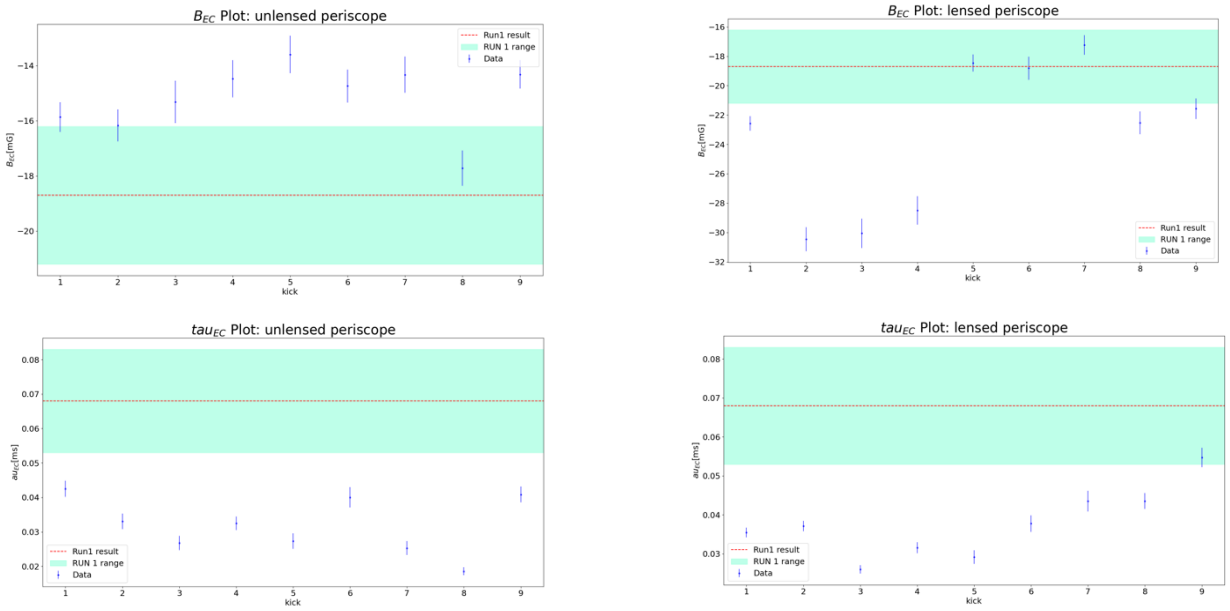

(a) (b)

Figure 26. For each picture 9 means average. Fig.26(a):On the top B_{EC} plot and at the bottom τ plot; red dashed line represents central RUN1 value while aquamarine range is the error bar: unlensed periscope. Fig.26(b):On the top B_{EC} plot and at the bottom τ plot; red dashed line represents central RUN1 value while aquamarine range is the error bar: lensed periscope.

However, the RUN1 general setting is different from ours and so this procedures could be meaningless. The important comparison is in term of ppb contribution on ω_a fit that, in general, doesn't depend on the setting chosen.

Following (2) we have to consider both spatial constraints and the time interval. A very rigorous way to take in account this fact is to perform an integral of our fit function over a certain space-time range. More precisely, the starting point of this calculus is the *5-parameters formula* for the distribution of the emitted positrons.

$$N(t) = N_0 e^{-\frac{t}{\tau}}(1 + Acos(\theta(t))$$

where I defined $\theta(t) = \int_0^t \omega(t)dt \propto \int_0^t B(t)dt$.

Our total magnetic field will be defined adding the main field and the transient field correction.

$$B(t) = B_0(1 + \frac{B_{EC}}{B_0} e^{-\frac{t}{\tau_{EC}}})$$

At the end of this calculus we finally get:

$$\theta(t) = cB_0\left(t + \frac{B_{EC}}{B_0} \cdot \tau_{EC} e^{-\frac{t}{\tau_{EC}}}\right) = \omega_a + \Delta\omega_a$$

where c is a constant prefactor and where we define $\Delta\omega_a = \frac{a_{EC}}{t} e^{-t/\tau_{EC}}$[3].

Averaging over a period T and dividing by ω_a we can find the quantity of our interest, that is $\frac{1}{\omega_a}\int_T a_{EC}\frac{e^{-t/\tau}}{t}\frac{dt}{T}$.

This can be simplified through a cruel approximation, getting, at the end, the following expression:

$$\frac{\Delta\omega_a}{\omega_a} \simeq \frac{B_{EC}}{B_{tot}} \times 8.5\% \times 0.94 \times \left(\frac{\tau_{EC}}{\tau_{EC} + \gamma\tau_\mu}\right)^2$$

From (2):

The kickers subtend about 8.5% of the storage ring azimuth, so the results were scaled by 0.085 to get the average kicker transient seen by the muons, assuming that the transients do not extend beyond the kicker plates. A weighted average of the muon distribution with this transient spatial dependence suggests the average muon sees a slightly smaller transient, reduced by a factor of 0.94. For a field perturbation of the form B(t) =B(t_0) exp[-(t - t_0)/τ_k], the fractional effect on the muon anomalous precession frequency for a fit starting at t = t_0 = 30μs and ending at measurement time t ≫ ($\gamma\tau_\mu$).

Plotting data as done for the parameters:

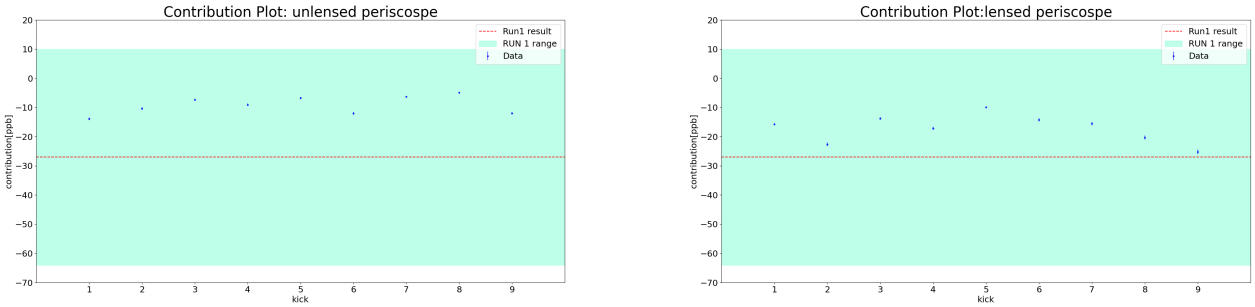

(a) (b)

Figure 27. Fig.27(a): contribution plot for unlensed periscope.Fig.27(b): contribution plot for lensed periscope

This results are clearly compatible with the RUN1 and the central values are even lesser! However,it is too early to draw conclusions because we are not considering systematic errors because of the difficulty to treat the noise. In this two plot we are just considering the errors resulting from uncertainties propagation so, for the moment, we can't conclude anything about an improvement in ppb contribution.

[3] the definition of the parameters comes from above

12. LOOKING AT THE FUTURE

Starting from October a new session with a new device will start and with its, a new data analysis. A new breadboard system has been built and should be easier than the previous one. Indeed it is composed by just the final part of the previous breadboard, namely the Wollaston prism and the two photodetector. There aren't any plates (and for this reason no scan is required) and the red light laser is inserted at the bottom of the periscope, avoiding in this way, the boring and hard alignment.

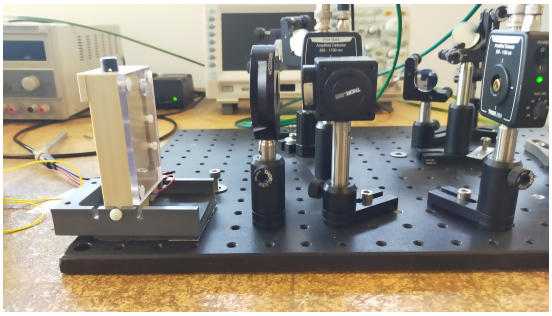

(a)

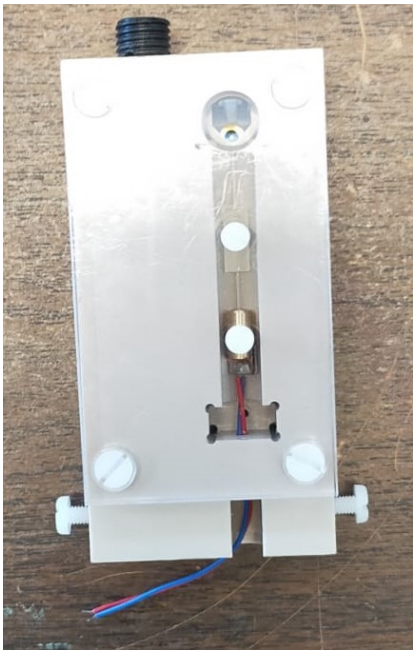

(b)

Figure 28. Fig.28(a):New breadboard schematic.Fig.28(b): New periscope: at the top we can see the red light laser

The great advantage of this set up is that it doesn't require any preliminary step and so we can start collecting data right away.

Hopefully, we will be able to save more time in order to focus only on data acquisition.

13. CONCLUSION

During this two months I have carried on my work both on Hardware and Software, trying to pull out results to the best of my skills. At the end, I can state that the work done confirms the results got with the fiber magnetometer during the RUN1 and, improving noise issues and the evaluation of the errors, we can make progresses in order to achieve a better understanding of this small,but non negligible, effect.

REFERENCES

[1] A.P. Schreckenberger et al.(2021),*The fast non-ferric kicker system for the Muon g-2 Experiment at Fermilab*, Nuclear Inst. and Methods in Physics Research, A 1011 (2021) 165597

[2] T. Albahri et al.(2021),*Magnetic-field measurement and analysis for the Muon g-2 Experiment at Fermilab*,Physical Review A 103, 042208 (2021)